SEPT Vibration Re-Test Report
Preliminary

V1.0

Prepared by:

R. Mueller-Mellin, University of Kiel

S. Boettcher, University of Kiel

J. Falenski, University of Kiel

L. Duvet, ESTEC

Doc. No.: STEREO-ETKI-011b

November 2004

Table of contents

1 Objectives

The purpose of this document is to give a preliminary analysis of the results of the SEPT vibration re-test which occurred at ESA/ESTEC from November 20 to 23, 2004. An official report (RD1) will be issued later by the facility.

The original vibration test was carried out at ESA/ESTEC from February 16 to 24, 2004. The repetition was made necessary after several repair activities to recover from failures described in IMPACT Problem Reports

- PR-7001 SEPT-DoorOpening 2004-02-20
- PR-7002 SEPT-Detector 2004-03-05
- PR-7003 SEPT-Pinpuller 2004-03-10
- PR-7004 SEPT-Accident 2004-05-04
- PR-7005 SEPT-Counting 200410-10

The test was performed according to the procedures specified in the SEPT Vibration Re-Test Plan (AD1).

2 Applicable Documents

AD1	SEPT Vibration Re-Test Plan, STEREO-ETKI-005-b, November 2004
AD2	SEPT Comprehensive Performance Test, STEREO-ETKI-009, January 2004
AD3	STEREO Environment Definition, Observatory, Component and Instrument Test Requirements Document, Doc. No. 7381-9003
AD4	STEREO Contamination Control Plan, Doc. No. 7381-9006
AD5	IMPACT Environmental Test Plan, Version D 2003-Dec-30
AD6	IMPACT Contamination Control Plan, Version A 2003-May-14
AD7	SEPT Vibration Test report Preliminary, STEREO-ETKI-011, February 2004

3 Reference Documents

RD1	SEPT FM Vibration Re-Test Facility Data Report, to be released
RD2	SEPT FM Vibration Test Facility Data Report ETS/REP/MECH/993, 17-03-2004
RD3	STEREO SEPT Structural Analysis TOS-MCS/2002/721/ln, January 2003
RD4	Validation of Force Limited Vibration Testing at NASA Langley Research Center, C.E. Rice, R. D. Buehrle, NASA/TM-2003-212404, May 2003
RD5	Reduction of Overstesting during vibration tests of space hardware, Y. Soucy, A. Cote, Vol. 48, No. 1, March 2002, Canadian Aeronautics and Space Journal

4 Acronyms and Abbreviations

EGSE	Electrical Ground Support Equipment
FPGA	Field Programmable Gate Array
PDFE	Particle Detector Front End
PIPS	Passivated Ion-implanted Planar Silicon detector
PSD	Power Spectrum Density
SEPT-E	Solar Electron and Proton Telescope – Ecliptic
SEPT-NS	Solar Electron and Proton Telescope – North/South
SSD	Solid State Detector

5 Overview

5.1 Set-up

The shaker is located at ESA/ESTEC (Netherlands) and is shown in Fig. 1:

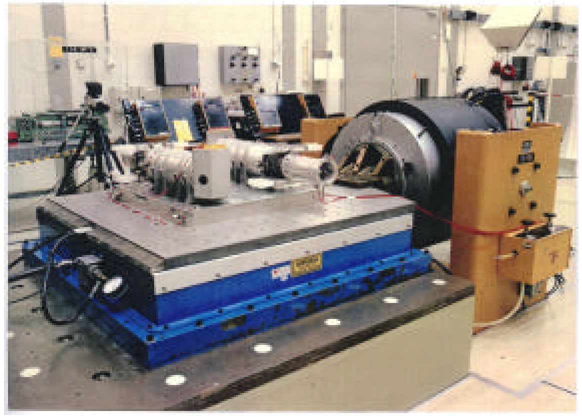

Figure 1:

70 kN shaker in the horizontal position (also known as 80 kN shaker after electrical refurbishment)

For the SEPT vibration tests, the configuration was as follows:

- The 70 kN shaker was placed in a vertical position (w.r.t. the position shown in Fig. 1)
- An aluminium cube of ~ 250 mm side length was used to support two flight units in one run
- By changing the faces on which the units are mounted, a different axis was stimulated
- No counterweight was used
- SEPT-E with Ultem bushings was mounted to the cube with fasteners M4 V2A, torque 2.6 Nm, mass 770g
- SEPT-NS with Ultem bushings was mounted to the bracket which in turn was mounted to the cube with fasteners M5 V2A, torque 5.1 Nm, mass 1110 g.

Two tri-axial accelerometers were used per unit, one placed on the sensor head (TP1), one placed on the electronics box (TP2). They were glued on Kapton tape placed in identical positions on all four units: on the SEPT rear side, i.e. opposite to the MDM connector side (see Fig. 2 and 3). The shaker is controlled via dedicated accelerometers attached to the adapter cube (pilot P1 and P2, co-pilots CP1 and CP2).

The instruments were constantly single-bagged during vibration runs and double-bagged during set-up periods (see Fig. 4, 5, and 6). Flaps in the inner bags allowed comprehensive performance testing between axes without removal of the inner bags. For transport between the shaker facility and the clean bench, where the CPTs were carried out, the units were enclosed in a custom made plexiglass container protected in an aluminium box.

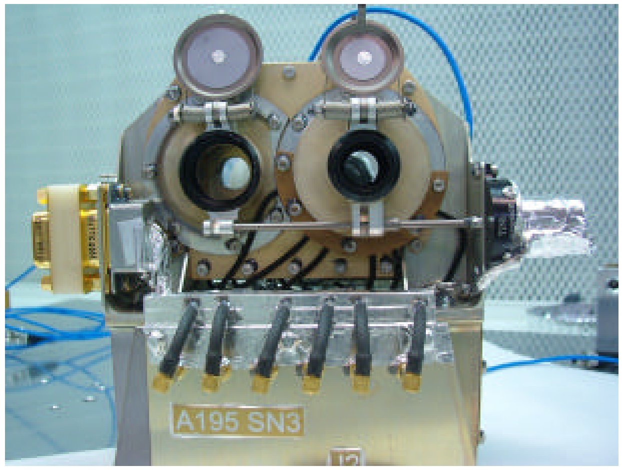

Figure 2:

Front view of SEPT-E FM2 (during door opening test prior to vibration) with accelerometers attached. Visible are detector (left aperture) and foil (right aperture).

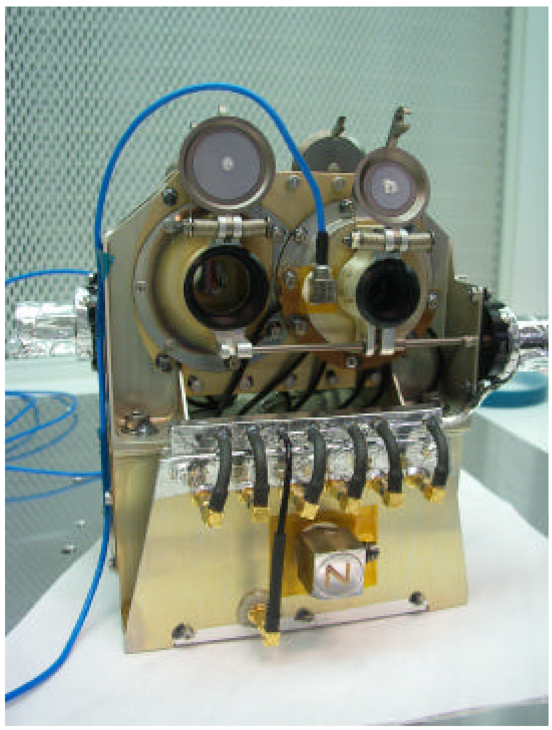

Figure 3:

Rear view of SEPT-E FM2 (during door opening test prior to vibration) with accelerometers attached (TP1 on sensor, TP2 on E-Box).

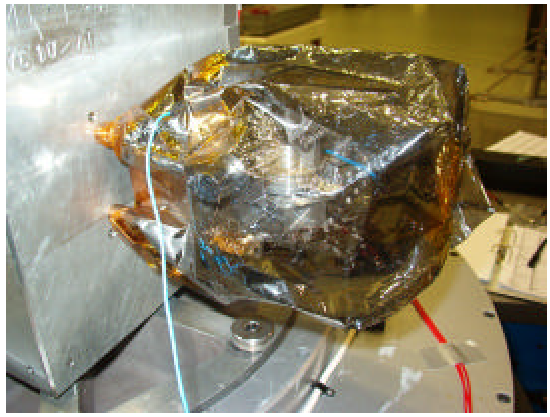

Figure 4:

SEPT-E FM1 mounted on adaptor cube for X-axis vibration

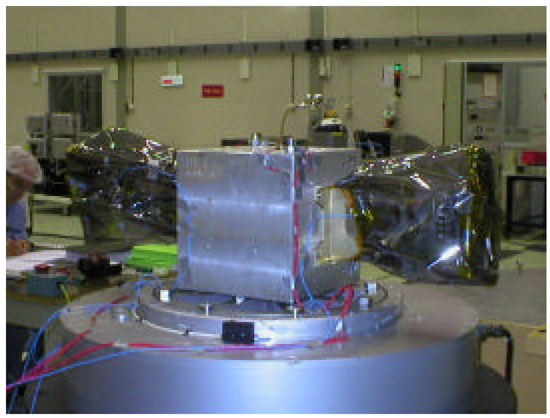

Figure 5:

SEPT-NS FM1 and FM2 mounted on adapter cube for Y-axis vibration

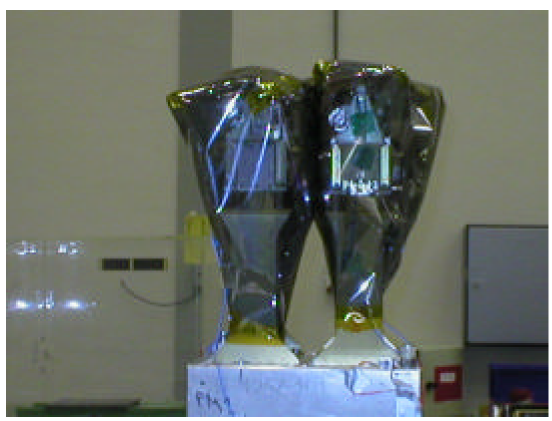

Figure 6:

SEPT-NS FM1 and FM2 mounted on adapter cube for Z-axis vibration

5.2 Axis definition

The sketches in Fig. 7 show the definition of the three instrument axes.

SEPT-E

SEPT-NS

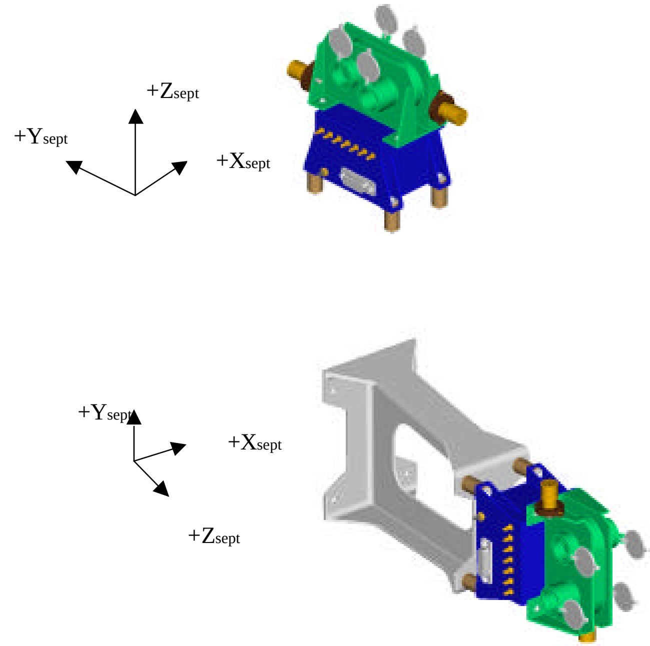

Figure 7: SEPT axis definition

5.3 *Test sequence*

The test levels as defined in AD3 and specified in AD1 were applied. The test sequence is shown in Table 2.

Run #	Data log name	Level	Unit and axis	Location on cube
1	FM1-E-SL-X-1 FM2-E-SL-X-1	Sine-Low 0.25 g	FM1 SEPT-E Xsept FM2 SEPT-E Xsept	Opposite lateral faces
2	FM1-E-ST-X FM2-E-ST-X	Sine-Thrust 16 g	FM1 SEPT-E Xsept FM2 SEPT-E Xsept	Opposite lateral faces
3	FM1-E-RPar-X FM2-E-RPar-X	Random-Parallel 7.4 g_{rms}	FM1 SEPT-E Xsept FM2 SEPT-E Xsept	Opposite lateral faces
4	FM1-E-SL-X-3 FM2-E-SL-X-3	Sine-Low 0.25 g	FM1 SEPT-E Xsept FM2 SEPT-E Xsept	Opposite lateral faces

Run #	Data log name	Level	Unit and axis	Location on cube
5	FM1-E-SL-Y-1 FM2-E-SL-Y-1	Sine-Low	FM1 SEPT-E Ysept FM2 SEPT-E Ysept	Opposite lateral faces
6	FM1-E-ST-Y FM2-E-ST-Y	Sine-Thrust 16 g	FM1 SEPT-E Ysept FM2 SEPT-E Ysept	Opposite lateral faces
7	FM1-E-RPar-Y FM2-E-RPar-Y	Random-Parallel 7.4 g_{rms}	FM1 SEPT-E Ysept FM2 SEPT-E Ysept	Opposite lateral faces
8	FM1-E-SL-Y-3 FM2-E-SL-Y-3	Sine-Low	FM1 SEPT-E Ysept FM2 SEPT-E Ysept	Opposite lateral faces

Run #	Data log name	Level	Unit and axis	Location on cube
9	FM1-E-SL-Z-1 FM2-E-SL-Z-1	Sine-Low	FM1 SEPT-E Zsept FM2 SEPT-E Zsept	Both units on top face
10	FM1-E-SLat-Z FM2-E-SLat-Z	Sine-Lateral 12 g	FM1 SEPT-E Zsept FM2 SEPT-E Zsept	Both units on top face
11	FM1-E-RPerp-Z FM2-E-RPerp-Z	Random-Perpendicul. 10.4 g_{rms}	FM1 SEPT-E Zsept FM2 SEPT-E Zsept	Both units on top face
12	FM1-E-SL-Z-3 FM2-E-SL-Z-3	Sine-Low	FM1 SEPT-E Zsept FM2 SEPT-E Zsept	Both units on top face

Run #	Data log name	Level	Unit and axis	Location on cube
13	FM1-NS-SL-X-1 FM2-NS-SL-X-1	Sine-Low	FM1 SEPT-NS Xsept FM2 SEPT-NS Xsept	Opposite lateral faces
14	FM1-NS-SLat-X FM2-NS-SLat-X	Sine-Lateral 12 g	FM1 SEPT-NS Xsept FM2 SEPT-NS Xsept	Opposite lateral faces
15	FM1-NS-RPar-X FM2-NS-Rpar-X	Random-Parallel 7.4 g_{rms}	FM1 SEPT-NS Xsept FM2 SEPT-NS Xsept	Opposite lateral faces
16	FM1-NS-SL-X-3 FM2-NS-SL-X-3	Sine-Low	FM1 SEPT-NS Xsept FM2 SEPT-NS Xsept	Opposite lateral faces

Run #	Data log name	Level	Unit and axis	Location on cube
17	FM1-NS-SL-Y-1 FM2-NS-SL-Y-1	Sine-Low	FM1 SEPT-NS Ysept FM2 SEPT-NS Ysept	Opposite lateral faces
18	FM1-NS-ST-Y FM2-NS-ST-Y	Sine-Thrust 16 g	FM1 SEPT-NS Ysept FM2 SEPT-NS Ysept	Opposite lateral faces
19	FM1-NS-RPar-Y FM2-NS-Rpar-Y	Random-Parallel 7.4 g_{rms}	FM1 SEPT-NS Ysept FM2 SEPT-NS Ysept	Opposite lateral faces
20	FM1-NS-SL-Y-3 FM2-NS-SL-Y-3	Sine-Low	FM1 SEPT-NS Ysept FM2 SEPT-NS Ysept	Opposite lateral faces

Run #	Data log name	Level	Unit and axis	Location on cube
21	FM1-NS-SL-Z-1 FM2-NS-SL-Z-1	Sine-Low	FM1 SEPT-NS Zsept FM2 SEPT-NS Zsept	Both units on top face
22	FM1-NS-SLat-Z FM2-NS-SLat-Z	Sine-Lateral 12 g	FM1 SEPT-NS Zsept FM2 SEPT-NS Zsept	Both units on top face
23	FM1-NS-RPerp-Z FM2-NS-RPerp-Z	Random-Perpendicul. 10.4 g_{rms}	FM1 SEPT-NS Zsept FM2 SEPT-NS Zsept	Both units on top face
24	FM1-NS-SL-Z-3 FM2-NS-SL-Z-3	Sine-Low	FM1 SEPT-NS Zsept FM2 SEPT-NS Zsept	Both units on top face

Table 2: Test sequence

6 Results

6.1 Overview

- The tests were performed according to the plan (AD1).
- All test levels were reached as specified.
- Comparison with test data from the first vibration campaign showed nearly perfect agreement.
- The CPTs between axes and after vibration showed nominal performance for all four units.
- The actuator test before vibration showed nominal performance for all four units.
- The actuator test after vibration showed nominal performance for SEPT-E FM1, SEPT-E FM2, SEPT-NS FM1, but failed for SEPT-NS FM2 (for details see below).

6.2 Active Notching

For safety reasons, active notching was installed for random vibration. Active notching consists of observing in real time the output PSD and limiting it to a chosen value in a narrow frequency band. A notch level of 90 g^2/Hz was chosen on the basis of measurements during the first vibration test campaign in February 2004 (see RD2) and using safety margin factors as discussed in the structural analysis (see RD3). From the test results it is difficult to see whether an actual notching had occurred, since the natural shaker uncertainty is of the same order of magnitude. There is a slight indication of notching at the resonance frequency (e.g. at 420 Hz for SEPT-E X-axis) which meets, however, well the requirement that test levels be maintained within ± 3 dB of nominal test levels over the test frequency range (see AD3).

6.3 Failure to open doors for SEPT-NS FM2

When attempting to open the doors on the rear side of SEPT-NS FM2 (i.e. side A) the pin-puller retracted correctly drawing 0.8 A for 45 ms as expected. However, both doors did not swing open, because the rod was still partly blocking the door clevises (see Fig. 8). Apparently, during vibration, the rod had loosened from the pinpuller pin because the rod was not sufficiently torqued into the pin tip which provides an internal thread. Inspection of side B showed an identical failure, so it was no attempted to open side B (see Fig. 9).

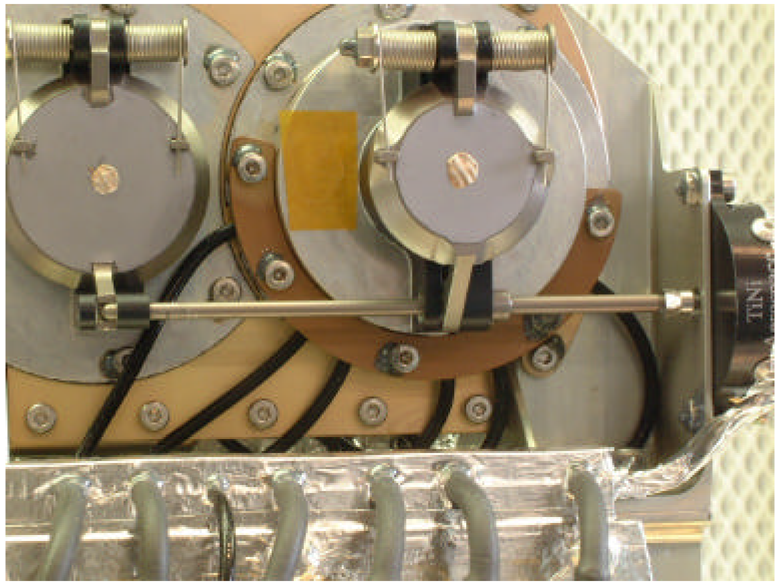

Figure 8: SEPT-NS FM2 side A after pin-puller actuation after vibration

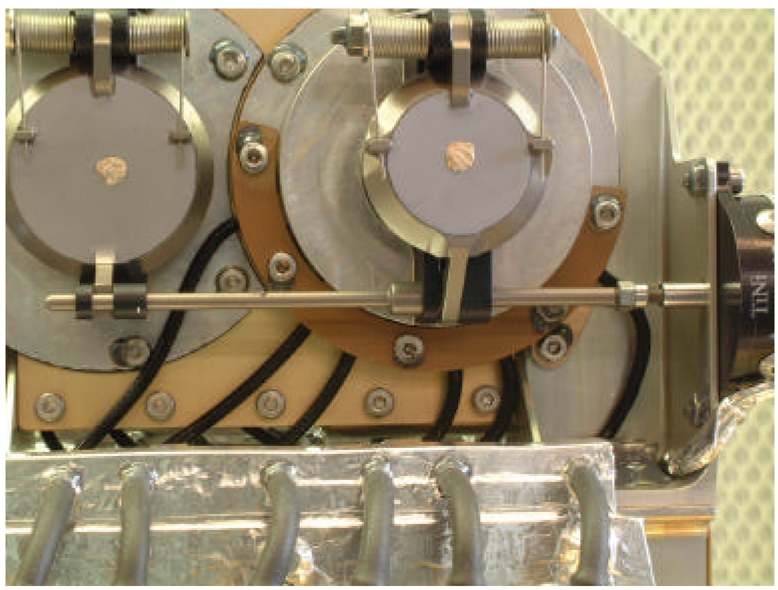

Figure 9: SEPT-NS FM2 side B after vibration, pin-puller actuation not attempted

This thread was not staked prior to vibration for the fear of losing a pin-puller in case of a disassembly later-on for some unexpected reason. As the mechanical specification from the manufacturer TiNi of the torque load was not clear to us ("nominal stress of 50 ksi stress"), the rod was torqued to good engineering practise only. An earlier attempt to apply adhesive on the rod/pin interface on the outside surface was discarded because this interface will move right to the hole drilled into the sensor mounting lug through which the pin is retracting.

The pin-puller of side A was re-stowed, the pin-puller rods of sides A and B were re-torqued to good engineering practise, the pin-pullers were actuated and the doors opened nominally with expected currents and activation times.

Having advanced thus far in the assembly and test program, we felt that it was justified to stake the thread on the pin-puller rods using Araldite 2014 adhesive. It was decided to stake all pin-puller-rods, even those who performed flawlessly after vibration. The SEPT materials list was updated to include Araldite 2014. A problem/failure report was issued (IMPACT PR-7006 SEPT-Rod .The four SEPT units proceeded to TV testing with staking applied.

6.4 Test Data

The basic results as measured at the sensor accelerator TP1 are given in Table 3.

Unit	Axis	Sine sweep		Random
		1st Resonance (Hz)	Max g	Max g rms
SEPT-E FM1	X	420	20.6	42.5
	Y	480	10.4	23.5
	Z	1200	8.05	29.7
SEPT-E FM2	X	420	19.7	42.6
	Y	480	6.18	16.7
	Z	1200	6.47	30.2
SEPT-NS FM1	X	116	10.3	20.8
	Y	250	5.67	20.3
	Z	730	5.39	39.7
SEPT-NS FM2	X	116	16.6	23.9
	Y	250	10.3	27.1
	Z	720	4.75	41.1

Table 3: Main results

The mechanical behaviour of the four SEPT units during re-vibration followed closely the performance during the first vibration campaign (cf. AD7 and RD2). A complete data set volume will be released both electronically and as hardcopy by the test facility (RD1).

7 Conclusion

The four SEPT units were tested according to AD1. Both sine and random vibration test runs were successful. Comparison of the two low level sine sweeps (before and after full level sine and full level random vibration) showed no major discrepancies, i.e. no mechanical damage could be detected in the frequency response. Comparison with test data from the first vibration campaign showed nearly perfect agreement, i.e. we have tested the same units!

CPTs carried out after each axis showed nominal performance. These CPTs included radioactive source tests to check on detector aliveness.

One unit failed during the door opening test after vibration. However, the cause of the failure was clearly and unambiguously diagnosed. The doors opened flawlessly after re-torquing.
A problem failure report was issued. Remedial measure was taken and considered satisfactory, pending approval by the FRB.

With all doors open, the foils and front detectors could be inspected. No damage was visible.